PLOS ONE

RESEARCH ARTICLE

Cell type-specific differences in redox regulation and proliferation after low UVA doses

Sylwia Ciesielska[1], Patryk Bil[1], Karolina Gajda[1], Aleksandra Poterala-Hejmo[1], Dorota Hudy[1], Joanna Rzeszowska-Wolny[1]*

1 Biosystems Group, Institute of Automatic Control, Silesian University of Technology, Gliwice, Poland

* joanna.rzeszowska@polsl.pl

OPEN ACCESS

Citation: Ciesielska S, Bil P, Gajda K, Poterala-Hejmo A, Hudy D, Rzeszowska-Wolny J (2019) Cell type-specific differences in redox regulation and proliferation after low UVA doses. PLoS ONE 14(1): e0205215. https://doi.org/10.1371/journal.pone.0205215

Editor: Markus M Bachschmid, Boston University, UNITED STATES

Received: September 18, 2018

Accepted: January 4, 2019

Published: January 25, 2019

Data Availability Statement: All relevant data are within the manuscript and its Supporting Information files.

Funding: This work was supported by the Polish National Science Center Grant #2015/19/B/ST7/02984. The funders had no role in study design, data collection and analysis, decision to publish, or preparation of the manuscript.

Competing interests: The authors have declared that no competing interests exist.

Abstract

Ultraviolet A (UVA) radiation is harmful for living organisms but in low doses may stimulate cell proliferation. Our aim was to examine the relationships between exposure to different low UVA doses, cellular proliferation, and changes in cellular reactive oxygen species levels. In human colon cancer (HCT116) and melanoma (Me45) cells exposed to UVA doses comparable to environmental, the highest doses (30–50 kJ/m^2) reduced clonogenic potential but some lower doses (1 and 10 kJ/m^2) induced proliferation. This effect was cell type and dose specific. In both cell lines the levels of reactive oxygen species and nitric oxide fluctuated with dynamics which were influenced differently by UVA; in Me45 cells decreased proliferation accompanied the changes in the dynamics of H_2O_2 while in HCT116 cells those of superoxide. Genes coding for proteins engaged in redox systems were expressed differently in each cell line; transcripts for thioredoxin, peroxiredoxin and glutathione peroxidase showed higher expression in HCT116 cells whereas those for glutathione transferases and copper chaperone were more abundant in Me45 cells. We conclude that these two cell types utilize different pathways for regulating their redox status. Many mechanisms engaged in maintaining cellular redox balance have been described. Here we show that the different cellular responses to a stimulus such as a specific dose of UVA may be consequences of the use of different redox control pathways. Assays of superoxide and hydrogen peroxide level changes after exposure to UVA may clarify mechanisms of cellular redox regulation and help in understanding responses to stressing factors.

Introduction

Ultraviolet radiation is the non-ionizing part of the electromagnetic radiation spectrum with a wavelength of 100–400 nm, invisible to human sight. The sun is a natural emitter of UV divided into three main fractions UVA (315–400 nm), UVB (280–315 nm), and UVC (100–280 nm), but most of this radiation is blocked by the atmosphere [1,2]. UVA constitutes the largest part (~95%) of UV radiation that reaches the Earth's surface [3], whereas UVB represents only 4–5% [1]. In irradiated humans UVA reaches the dermis and hypodermis and has

no direct impact on DNA, but it can influence cellular structures indirectly by induction of reactive oxygen species (ROS) which can damage macromolecules [1, 4]. For a long time UV was regarded as damaging for cells and organisms [5], but since a few decades it is known that low doses can also stimulate proliferation of cells; however, the mechanisms underlying this phenomenon are not completely understood [1, 3, 6, 7].

Studies of signaling pathways in conditions where UVA stimulates cell proliferation show changes in the levels of proteins engaged in controlling proliferation such as cyclin D1 [8,9], Pin1 [3], and Kin17 [10] or activation of epidermal growth factor receptor (EGFR) which is strongly mitogenic in many cell types [8]. Experiments on mice showed that UVA can accelerate tumor growth [2,11].

One effect of exposure to UV is induction of ROS in cells, including different reactive molecules and free radicals derived from molecular oxygen [12] which together with reactive nitrogen species (RNS) play important roles in regulation of cell signaling and survival (reviewed in [13]). ROS can exert opposing effects, inducing cell damage and death or stimulating proliferation by protein modifications and participation in signaling pathways [14–23]. Many complex mechanisms guard redox homeostasis, the balance between generation and elimination of ROS and antioxidant systems, such as superoxide dismutase, catalase or glutathione peroxidases which participate in these control systems [22, 24]. The role of ROS in stimulating proliferation by low doses of UVA was supported by experiments in which irradiation with a low-power diode laser increased ROS production accompanied by increased cell proliferation which was prevented by addition of catalase or superoxide dismutase [9], suggesting that ROS are at least partly involved in stimulating proliferation [19]. ROS in cells originate both from external sources and as byproducts of cellular processes [9, 20, 21, 24]. Low levels of ROS stimulate cell proliferation by activating signaling pathways connected with growth factors, causing increased cell cycle progression, while higher levels show toxic effects causing cell death or senescence [24, 25]. RNS include nitric oxide (NO), a highly reactive gas synthesized from L-arginine by members of the nitric oxide synthase (NOS) family [26]. NO modulates many cellular functions [27] by acting as a messenger for paracrine and autocrine communication and its production and degradation are strictly controlled in different cell types [28]. All cells of multicellular organisms produce superoxide and NO, which appear to be the main radicals responsible for the regulation of cellular redox homeostasis. This regulation is especially important in the presence of external ROS sources, because cells do not distinguish between endogenously- and exogenously-generated ROS. The main endogenous sources of superoxide are electron leakage from the mitochondrial respiratory chain and NADPH oxidases (NOXs), a family of enzymes dedicated to the production of ROS in a variety of cells and tissues [20, 29, 30]. The generation of superoxide is highly conserved across all eukaryotic life and is strictly regulated by antioxidant enzymes and reducing agents [13, 29], and the fluctuating level of ROS in cells has been postulated to be an important mechanism regulating progression through the cell cycle [20, 22, 31, 32].

The aim of the study is to investigate the basal mechanisms of redox regulation in cells. As ROS and NO play an important role in many intra- and inter-cellular signaling pathways, participate in regulation of the cell cycle (reviewed in [20]), and show increased levels after UV radiation [4] we have studied if and how changes in their levels in irradiated cells could be related to the effects of UVA on proliferation, using human melanoma (Me45) and colon cancer (HCT116) cells irradiated with UVA. We show that some low doses, specific for each cell line, stimulate clonogenic survival whereas other, even lower doses inhibit proliferation. Comparison of the changes in the intracellular levels of ROS, NO, and superoxide (O_2^-) after irradiation with stimulating, suppressing, or neutral UVA doses suggests that these cell lines

regulate their ROS levels by different pathways, and that it is the dynamics of superoxide or H_2O_2 levels which plays a crucial role in growth stimulation or inhibition.

Materials and methods

Cell lines and culture

Human melanoma cells (Me45, established in the Center of Oncology in Gliwice from a lymph node metastasis of skin melanoma; [33]) and human colorectal carcinoma cells (HCT116; p53+/+, ATCC) were maintained in DMEM/F12 medium (PAN Biotech. Aidenbach, Germany, cat, #P04-41150) enriched with 10% fetal bovine serum (EURx, Gdansk, Poland cat# E5050-03-500) at 37 ˚C in a humidified atmosphere enriched in 5% CO_2. The cells, 1000–5000 per dish, were irradiated at room temperature (21˚C) in culture plates (Sarstedt, Numbrecht, Germany cat# 83.3900) (covers opened) with various doses (0.05–50 kJ/m^2) of UVA (365 nm) generated by a UV crosslinker (model CL-1000, UVP, Upland, CA, USA). Time of exposition was 1.15 seconds for any 0.05 kJ/m^2 (i.e. 1.15 seconds for 0.05 kJ/m^2, 23 seconds for dose of 1 kJ/m^2). Untreated cells were used as a control.

Clonogenic survival asssays

Control and irradiated cells were seeded in 60-mm dishes at 1000–5000 cells/dish and incubated from 5 to 14 days (depending on the cell line) at 37˚C in a humidified atmosphere. The colonies were fixed with 2 ml cold 96% ethanol for 3 min, than washed with PBS (PAN Biotech., Aidenbach, Germany, cat. no. P04-36500) and stained with 0.5% methylene blue in 50% ethanol. Cells in colonies containing more than 50 cells (estimated under the microscope) were counted and the surviving fraction was calculated as the plating efficiency of irradiated cells relative to that of control un-irradiated cells.

Intracellular reactive oxygen species levels

To quantitate intracellular ROS, 100.000 cells were seeded, growing cells were collected by trypsinization, suspended in culture medium to which 2',7'-dichlorofluorescein diacetate (DCFH-DA; Sigma-Aldrich, St. Louis, USA, Cat#287810) was added to final concentration of 30μM. Cells were incubated for 30 min at 37˚C in the dark, washed with medium, suspended in PBS, and kept for 15 min on ice in the dark. Fluorescence was measured by flow cytometry (Becton Dickinson FACS Canto) using the FITC configuration (488 nm laser line, LP mirror 503, BP filter 530/30), usually 10,000 cells were assayed per sample. To assess superoxide radicals in living cells, MitoSox Red fluorogenic reagent (Thermo Fisher Scientific, Waltham, USA, cat. no. M36008) was used [34, 35]. Cells were collected, suspended in medium (20,000 cells/300μl), incubated with MitoSox Red (5 μM final concentration) for 20 min at 37˚C in the dark, and washed and resuspended in PBS. Samples were kept on ice until analysis by flow cytometry (Becton Dickinson FACS Canto, 488 nm laser line, LP mirror 566, BP filter 585/42), measuring 10,000 cell per sample. To assess NO, cells were incubated with 1μM 4-amino-5-methylamino-2',7'-difluorescein diacetate (DAF-FM, Thermo Fisher Scientific, Waltham, USA, cat.# D23844) for 30 min in dark conditions at 37˚C and washed with PBS. The fluorescence intensity of 10,000 cells was measured by flow cytometry using the FITC configuration (488 nm laser line. LP mirror 503, BP filter 530/30).

Results are expressed as mean fluorescence intensities ±SD from three independent experiments.

Fluorescence microscopy and image analysis

Fluorescent microscopy assays of superoxide and NO were performed with the same fluorescent reagents as for cytometry (MitoSOX Red and DAF-FM diacetate, Thermo Fisher Scientific, Waltham, USA). HCT116 and Me45 cells were seeded at 10,000 cells per well in 4-well cell culture chambers (Sarstedt, Numbrecht, Germany, cat# 94.6140.402), grown in DMEM medium supplemented with 10% fetal bovine serum for 24 hours at 37˚C in standard conditions, and labelled with MitoSOX Red (2.5μM) in the first well, DAF-FM Diacetate (2.5μM) in the second well, both dyes in the third well, and no dye in the last (control) well. Cells were incubated for 20 minutes at 37˚C in a humidified atmosphere enriched with 5% CO_2, the culture medium was removed, the cells were washed with PBS, fixed with 0.5 ml of cold 70% ethanol per well for 10 minutes, and washed with the same volume of deionized water for 3 minutes. Slides with fixed cells were covered with mounting gel and a cover glass. Images were captured with an Olympus BX43 microscope with a 40x objective and a CoolLED precisExcite fluorescence excitation system. Red and green fluorescence and transparent light images were obtained for 10 areas containing cells stained with both fluorescent dyes on each slide and analyzed with Matlab 2016b software using the functions corrcoef and scatter to detect correlation between the values of corresponding pixels in both fluorescence images.

Expression of genes coding for proteins engaged in cellular redox processes

We identified 574 genes which are directly or indirectly engaged in redox processes, using GO terms such as oxide, superoxide, nitric oxide, hydrogen peroxide, ROS and reactive oxygen species. The levels of transcripts of these genes in non-irradiated HCT116 and Me45 cells were extracted from our earlier Affymetrix microarray experiments [17, 32] whose results are available in the ArrayExpress database under accession number E-MEXP-2623. All data are MIAME compliant. Microarray data quality was assessed using simpleaffy Bioconductor package [36]. Raw HG-U133A microaarray data obtained from two experiments, based on Me45 and HCT116 cell lines, were processed using Brainarray EntrezGene specific custom CDF (v22) [37] in RMAexpress program [38] using PLM (Probe Level Model) normalization method. Biological replicates were averaged and expression levels compared between Me45 and HCT116 cell lines. We extracted all genes which showed at least 1.2-fold difference for further study.

Assay of total and oxidized glutathione levels

For assays of total glutathione we used Rahman et al.'s modification [39] of the colorimetric assay originally proposed by Vandeputte et al. [40] which is based on the reaction of GSH with 5,5′-dithio-bis (2-nitrobenzoic acid) (DTNB, Sigma-Aldrich, Saint Louis, USA, cat# D-8130) which produces 5-thio-2-nitrobenzoic acid (TNB) and its adduct with oxidized glutathione (GS-TNB). The disulfide product was reduced by glutathione reductase (0.2 U) (Sigma-Aldrich, Saint Louis, USA, cat. no. G-3664)) in the presence of 0.8mM NADPH (Sigma-Aldrich, Saint Louis, USA, cat. no. D-8130). The TNB chromophore was measured at 412 nm in a microplate (96-plate) reader (Epoch, Biotek, Winooski, USA). For measurements of oxidized glutathione (GSSG) levels, cell extracts made by sonication in 0.1% Triton X-100 (Sigma-Aldrich, Saint Louis, USA, cat# T8787) and 0.6% sulfosalicylic acid (Sigma-Aldrich, Saint Louis, USA, cat# S-2130) in 0.05M potassium phosphate buffer pH 7.2 containing 1 mM EDTA (KPE) buffer were treated with 2-vinylpyridine (Sigma-Aldrich, Saint Louis, USA, cat# 132292) for 1 h at room temperature, excess 2-vinylpyridine was neutralized with triethanolamine (Sigma-Aldrich, Saint Louis, USA, cat# T1377), and the enzymatic recycling and reaction with DTNB was carried as described above.

Reverse transcription and real-time quantitative polymerase chain reaction (RT-qPCR)

RNA was extracted with Total RNA mini kits (A&A Biotechnology, Gdansk, Poland, cat# 031–100) and reverse transcribed using NG dART kits (Eurx, Gdansk, Polska, cat# E0801) using oligo(dT). RT-qPCR was performed on a BioRad CFX 96 System using the Real-Time 2x PCR Master Mix SYBR A kit (A&A Biotechnology, Gdansk, Poland, cat# 2008-100A). Reaction mixtures were incubated for 2 min at 50˚C, 4 min at 95˚C, followed by 50 cycles of 45 sec at 95˚C, and 30 sec at 54–60˚C (depending on the primer set). Levels of expression were estimated by the ΔCT method as in [15]. RPL41 transcript was used as reference. Sequences of primers for RT-qPCR were summarized in S1 Table Primers sequences were designed using Primer-BLAST [41] and checked with OligoAnalyzer Tool [42].

Statistical analyses

Results are expressed as means ± SD from at least three biological replicates. Two-sided Student's t-test was used for identification of statistically significant differences ($p < 0.05$) between UV-treated and control (untreated) cells. The standard deviation of expression levels were calculated from SD of the target and reference values using formula $SD = (SD_1^2+SD_2^2)^{1/2}$. Correlations between time course changes in irradiated and control cells were calculated using Pearson's test and are presented as correlation coefficients.

Results

UVA induced proliferation changes are dose and cell-type specific

HCT116 and Me45 cells were exposed to a range of UVA radiation doses (0.05, 0.1, 0.25, 0.5, 1, 5, 10, 15, 20, 30, 40, or 50 kJ/m^2) and their proliferation was studied by clonogenic tests. Some doses stimulated proliferation and others suppressed proliferation when compared to un-irradiated controls in both cell lines, although they responded differently and the doses that increased clonogenicity were specific for each cell line (Fig 1). HCT116 cells showed a statistically significant increase of colony formation after exposure to 10 kJ/m^2 (p-value 0.02) and a decrease after 0.1, 40, and 50 kJ/m^2 (p-values 0.02, 0.05 and <0.01). The clonogenicity of Me45 cells increased after irradiation with 1 and 10 kJ/m^2 (p-value <0.01) but was reduced after 15 to 50 kJ/m^2 (p-values 0.01, 0.01, 0.045, 0.04 and <0.01 respectively).

Low UVA doses do not significantly influence average levels of ROS

We used specific fluorescent probes and flow cytometry to compare the levels of ROS and NO in cells irradiated with different UVA doses with those in control cells. Fig 2 shows the effect of UVA on the level of superoxide detected by MitoSox, of NO detected by DAF-FM, and of ROS detected by DCFH-DA. The average values for each dose were calculated from all twelve assays performed in different experiments and at different time points.

Average superoxide levels showed a tendency to increase with higher UVA dose in both cell lines, but the increases were not statistically significant. NO levels did not change or decreased slightly with higher doses. The levels of ROS detected with DCFH-DA also did not change in irradiated HCT116 cells, but Me45 cells showed small irregular increases with lower doses and decreases with higher doses. This probe detects several different radicals and was first used for detection of H_2O_2 [43, 44], and it seems probable that the ROS changes detected by this probe mainly reflect changes of H_2O_2 levels. None of the differences in average levels of ROS or NO radicals between control and irradiated cells were statistically significant.

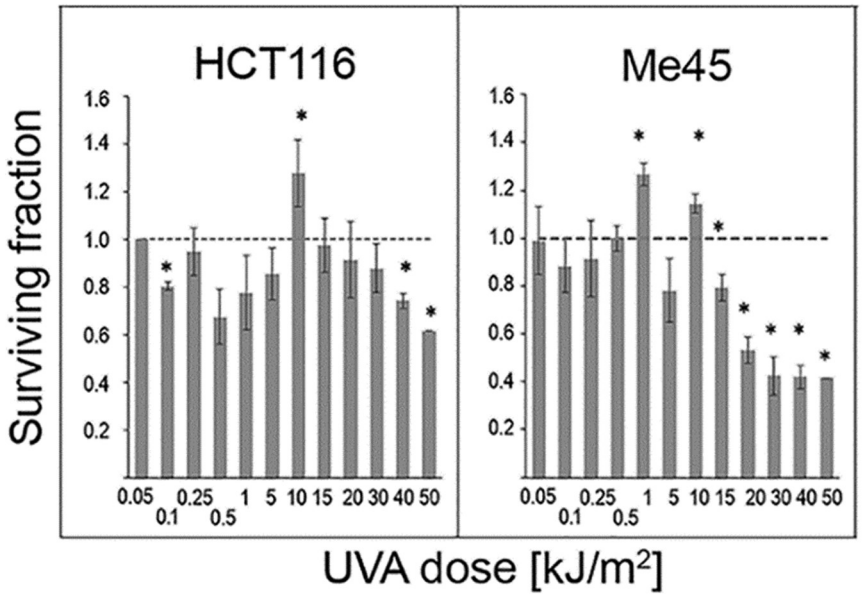

Fig 1. Clonogenicity of human cells after exposure to different UVA doses. (A) HCT116 cells, (B) Me45 cells. Data show the mean and SD of 3 experiments. Asterisks denote statistical significance of differences between irradiated and control samples with a p-value <0.05. The horizontal dashed line represents the control level.

https://doi.org/10.1371/journal.pone.0205215.g001

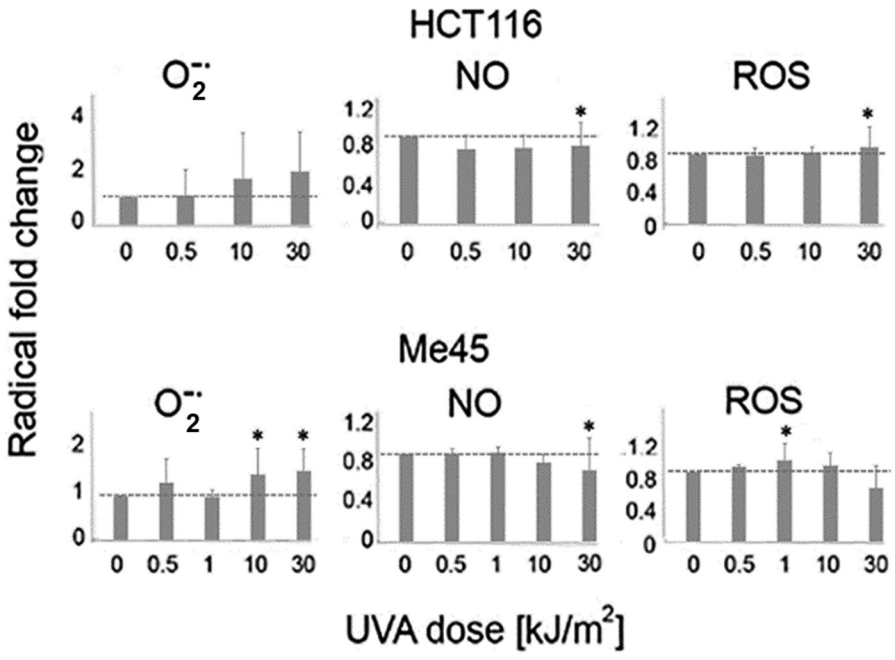

Fig 2. Average levels of ROS and NO in HCT116 and Me45 do not significantly change after exposure of cells to different UVA doses. The levels were measured four times during 24 h in control and cells irradiated with different UVA doses and experiment was repeated 4 times. The results are presented as fold change in irradiated cells versus non-irradiated controls. Data show the mean and standard deviation from 4 experiments; statistically significant differences ($p < 0.05$) were marked with an asterisks).

https://doi.org/10.1371/journal.pone.0205215.g002

ROS level dynamics change differently after different UVA doses

Although the UVA doses which we used did not change the average ROS levels significantly, they influenced fluctuations of these levels. The time course changes of the levels of ROS assayed by DCFH-DA, of superoxide, and of NO in cells irradiated with a particular dose or not irradiated are shown in Fig 3. Me45 and HCT116 cells responded to different doses with very different kinetics of radical levels and these dynamics of changes were cell type-specific. At first sight it is difficult to identify features which could be correlated with the increased or decreased clonogenic potential observed after irradiation with some doses.

To evaluate the similarity between radical dynamics in UVA-irradiated and control cells, we calculated correlation coefficients using Pearson's test. The dynamics of NO levels did not change significantly after exposure of cells to any of the UVA doses studied, and the increases and decreases appeared at similar time points in control and irradiated cells. The correlation coefficients between cells irradiated with different doses or not irradiated were >0.9 for HCT116 cells and >0.8 for three out of four doses in Me45 cells (Table 1). This positive correlation suggests that the changes of NO levels are strictly controlled in both cell lines after both stimulating or inhibiting proliferation UVA doses.

The superoxide level dynamics in Me45 cells irradiated with any dose were highly correlated with those in control cells (Table 1). In contrast, in HCT116 cells this level showed clear differences between the effects of UVA doses which stimulated or did not stimulate clonogenic potential; the dynamics of superoxide levels after doses inhibiting proliferation were inversely correlated with those in control cells, while after doses which stimulated proliferation these levels were positively correlated with those in control cells; however the correlation coefficients were rather low. The dynamics of the level of ROS in Me45 cells assayed by DCFH-DA changed after irradiation in a manner similar to those of superoxide in HCT116 cells, proliferation-inhibiting doses showing a negative correlation and proliferation-stimulating doses a positive correlation with the dynamics in control cells.

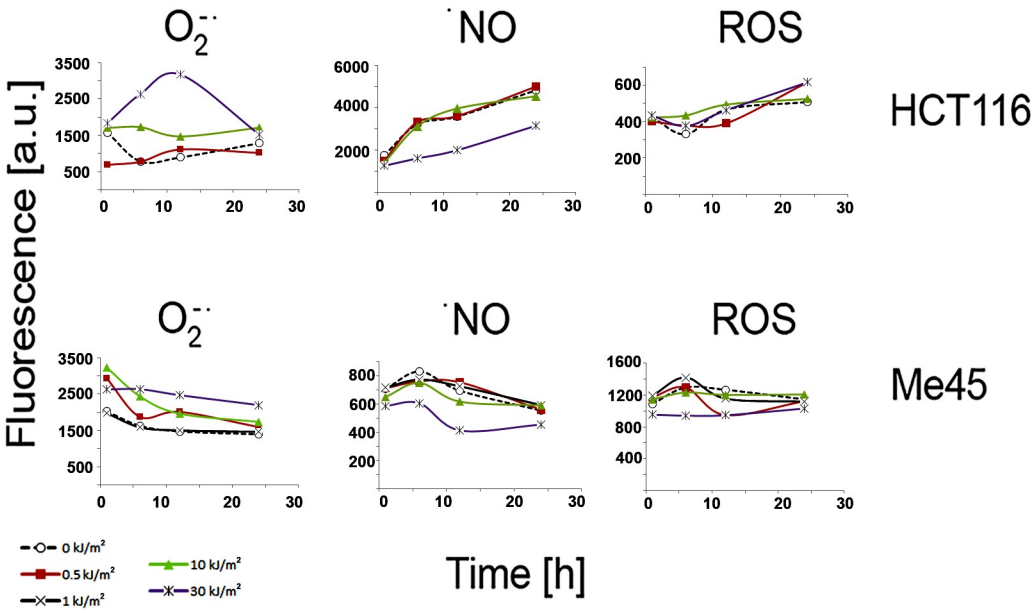

Fig 3. The dynamics of the levels of superoxide, nitric oxide and ROS detected by DCFH-DA in control and UVA irradiated cells. Each curve represents the results after exposure to a particular UV dose shown on the right; data are means from three experiments and error bars are not shown for clarity.

https://doi.org/10.1371/journal.pone.0205215.g003

Table 1. Correlation coefficients for the degree of similarity between radical dynamics in UV-irradiated vs. control cells.

	Superoxide[1]	ROS[2]	NO[3]
HCT116 cells			
0.5 kJ/m^2	**-0.38**	0.7	1*
10 kJ/m^2	0.37	0.81	0.97*
30 kJ/m^2	**-0.79**	0.88	0.94*
Me45 cells			
0.5 kJ/m^2	0.95*	**-0.01**	0.89*
1 kJ/m^2	0.99*	0.59	0.89*
10 kJ/m^2	0.99*	0.83	0.93*
30 kJ/m^2	0.98*	**-0.47**	0.67

[1]measured by MitoSox.

[2]detected by DCFH-DA (mainly H_2O_2).

[3]measured by DAF-FM;

*Pearson's correlation p-value <0.05. Bold values indicate changes from a positive to a negative correlation coefficient.

https://doi.org/10.1371/journal.pone.0205215.t001

HCT116 and Me45 cells differ in intracellular level and localization of NO and superoxide

Me45 cells had a ~5 times lower level of NO than HCT116 cells but higher levels of ROS detected by DCFH and of superoxide, as assayed by flow cytometry (Fig 4A). Analysis of single cells using fluorescence microscopy showed that in both cell types, most NO and superoxide were co-localized as shown by a high positive correlation of their signals in single pixels. Rare HCT116 cells contained larger regions with a high NO and a low superoxide signal (for example, Fig 4B) but similar regions were not seen in Me45 cells. Co-localization was significantly higher in Me45 than in HCT116 cells; Pearson's correlation coefficients for all pixels in 10 fields containing 5 to 10 cells were 0.9 and 0.6 in Me45 and HCT116 cells, respectively.

HCT116 and Me45 cells have different levels of some transcripts participating in redox systems

The differences in response to UVA and in radical levels in the two cell lines suggested that they use different mechanisms for the regulation of their redox status. To get more information on these mechanisms, we compared the expression of different genes coding for proteins engaged directly or indirectly in redox processes in each cell line. The expression levels of more than 500 candidate genes found on the basis of ontology terms were compared using our earlier microarray data for Me45 and HCT116 cells [17]. The full list of these genes and their expression levels are given in S2 Table of the Supplement. Both cell lines express many genes engaged in redox regulation and expression of some of these genes is significantly higher in Me45 or HCT116 cells (Tables 2 and 3). This cell line specific enrichment was observed also after UVA exposure in RT-qPCR experiments (Table 4, Fig 5).

Me45 cells contain lower levels of transcripts for thioredoxin (TXN) and peroxyredoxin (PRDX) and higher levels of transcripts for thioredoxin-inhibiting protein (TXNIP). On the other hand, genes coding for glutathione S-transferases (GST) show higher expression in Me45 cells, with the GSTM3 transcript showing the largest difference. Transcripts for

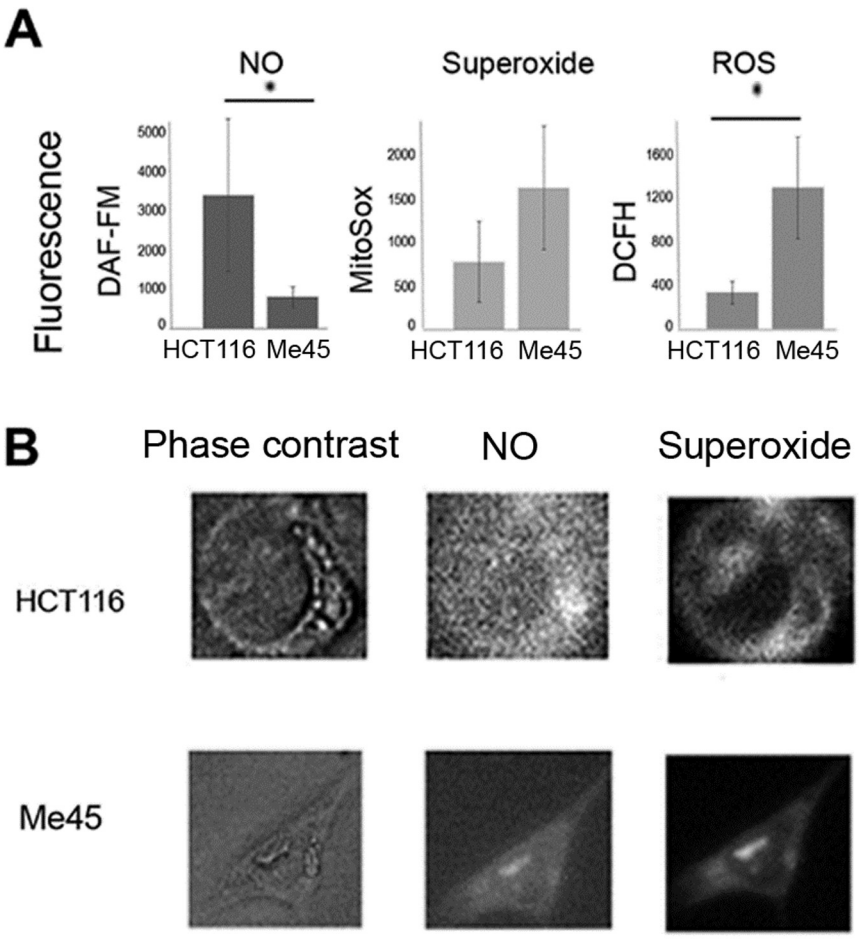

Fig 4. Nitric oxide and ROS in HCT116 and Me45 cells. A; mean levels of NO, superoxide and ROS detected by DAF-FM, MitoSOX Red and DCFH-DA respectively, measured in whole population of unirradiated cells by flow cytometry (data presented as a mean with a standard deviation from 4 experiments; statistically significant differences ($p < 0.05$) were marked with an asterisks), B; examples of superoxide and NO distribution in single HCT116 and Me45 cells observed by fluorescence microscopy, NO detected by fluorescence of DAF-FM diacetate and superoxide by MitoSOX Red.

https://doi.org/10.1371/journal.pone.0205215.g004

the antioxidant ATOX1, a copper chaperone which may increase activity of the protein SOD1 by providing copper ions and influence *SOD3* gene expression as a transcription factor [45, 46], are more than 10 times more abundant in Me45 than in HCT116 cells. There are also some genes which are significantly more highly expressed in HCT116 cells, for example GTP cyclohydrolase 1 which codes for the first and rate-limiting enzyme in biosynthesis of tetrahydrobiopterin (BH4), a cofactor required for activity of nitric oxide synthases [47, 48].

Glutathione in HCT116 and Me45 cells. Glutathione is an important player in cell redox regulation [39] and the gene *GCLM* which codes for glutamate-cysteine ligase regulatory subunit, required for synthesis of glutathione, is more highly expressed in HCT116 than in Me45 cells (Table 3). We therefore compared the levels of reduced (GSH) and oxidized (GSSG) glutathione in these cells. The levels of total glutathione, GSH (~96% of the total), and of GSSG were lower in Me45 cells, but the differences were not statistically significant (Fig 6).

Table 2. Genes with higher expression in Me45 than in HCT116 cells (microarray data).

Gene	Gene symbol	Transcript level [a.u.][1]	Enrichment[2]
Glutathione S-Transferase Mu 3	*GSTM3*	299	27.0
Antioxidant 1 Copper Chaperone	*ATOX1*	3336	11.3
Thioredoxin Interacting Protein	*TXNIP*	346	10.7
Glutathione S-Transferase Alpha 4	*GSTA4*	316	3.0
Peroxidasin	*PXDN*	80	2.8
Glutathione S-Transferase Kappa 1	*GSTK1*	734	2.4
SH3 Domain Binding Glutamate Rich Protein Like 3	*SH3BGRL3*	552	2.3
Cyclin Dependent Kinase 5	*CDK5*	565	2.2
Cyclin Dependent Kinase 2	*CDK2*	359	2
Glutathione S-Transferase Pi 1	*GSTP1*	1042	1.8
Catalase	*CAT*	402	1.6
Glutathione S-Transferase Omega 1	*GSTO1*	2037	1.4
Microsomal Glutathione S-Transferase 3	*MGST3*	1334	1.2
Thioredoxin Reductase 1	*TXNRD1*	758.2	1.1

[1]arbitrary units reflect normalized data from microarray experiment.

[2]Fold change

https://doi.org/10.1371/journal.pone.0205215.t002

Table 3. Genes with higher expression in HCT116 than in Me45 cells(microarray data).

Gene	Gene symbol	Transcript level[1]	Enrichment[2]
GTP Cyclohydrolase 1 (BH4 synthesis)	*GCH1*	260	19
Dimethylarginine Dimethylaminohydrolase 1 (demethylation of arginine)	*DDAH1*	279	11
F2R Like Trypsin Receptor 1	*F2RL1*	206	9
Thioredoxin Like 1	*TXNL1*	1281	4
Glutamate-cysteine ligase regulatory subunit (glutathione synthesis)	*GCLM*	170	3.4
NAD(P)H Quinone Dehydrogenase 2	*NQO2*	515	3
Thioredoxin Related Transmembrane Protein 1	*TMX1*	397	2.5
Peroxiredoxin 2	*PRDX2*	1448	2.5
Thioredoxin	*TXN*	2269	2.4
Glutaredoxin 5	*GLRX5*	976	2.4
Nitric oxide synthase interacting protein	*NOSIP*	299	2.4
Glutaredoxin 2	*GLRX2*	329	2.2
Peroxiredoxin 3	*PRDX3*	791	1.9
Peroxiredoxin 6	*PRDX6*	1009	1.8
LanC Like 1	*LANCL1*	241	1.7
Superoxide Dismutase 1	*SOD1*	2902	1.7
Peroxiredoxin 1	*PRDX1*	2571	1.5
Nitric Oxide Synthase 2	*NOS2*	74	1.5
Peroxiredoxin 4	*PRDX4*	1303	1.4
Glutathione Peroxidase 4	*GPX4*	1331	1.2
Apurinic/Apyrimidinic Endodeoxyribonuclease 1	*APEX1*	1545	2.7

[1]arbitrary units reflect normalized data from microarray experiment.

[2]Fold change

https://doi.org/10.1371/journal.pone.0205215.t003

Table 4. Enrichment of selected genes expression after UVA radiation (RT-qPCR).

Gene	Gene symbol	Enrichment[1]		
		Control	10 kJ/m^2	30 kJ/m^2
Genes with higher expression in HCT116 than in Me45 cells				
Glutathione Peroxidase 4	GPX4	7,7	1,7	5,7
Thioredoxin	TXN	2,0	1,2	1,1
Peroxiredoxin 3	PRDX3	2,6	2,2	2,5
Genes with higher expression in Me45 than in HCT116 cells				
Catalase	CAT	2,7	2,2	2,1
Glutathione S-Transferase Omega 1	GSTO1	3,0	2,8	3,1
Glutathione S-Transferase Pi 1	GSTP1	3,3	2,2	1,9

[1]Fold change

https://doi.org/10.1371/journal.pone.0205215.t004

Discussion

Stimulation of proliferation by UVA and fluctuations of intracellular ROS level

Stimulation of cell proliferation by UVA radiation at doses of 3–9 kJ/m^2 has been known for a few decades. [3,9]. Here we show that doses in this range, but not exceeding 10 kJ/m^2, increase the clonogenic potential of HCT116 and Me45 cells and that this effect is dose- and cell type-specific (Fig 1).

We assumed that the increase of surviving fraction observed upon exposition to some doses of UVA reflect induction of cell proliferation, rather than decrease in apoptosis as the basal apoptotic fraction in studied cells was very small (< 6%) and its decrease would not cause change significant enough to be detected by clonogenic survival assay.

We believe that this effect may be related to intracellular levels of ROS and RNS [34, 35], and supports a role for redox conditions, superoxide, and NO in regulation of proliferation which was suggested 30 years ago [14, 49, 50, 51, 52].

The levels of intracellular ROS, superoxide, and NO, assayed using specific probes, changed in time (Fig 3) in agreement with the fluctuations of ROS level observed by others and proposed to be important in regulation of the cell cycle (reviewed in [20]). In some cases the kinetics of the changes of level after irradiation were highly correlated with those in control cells (Table 1); for example, in both cell types the general pattern of NO level change did not vary after irradiation although their levels differed (Fig 3), suggesting that the pattern of NO level change is important for regulatory mechanisms in both cell types. For other radicals, the correlation between irradiated and control cells was much lower and sometimes changed sign; for example, in Me45 cells the fluctuations of superoxide level did not vary after irradiation and were highly correlated with those in control cells, whereas in contrast the fluctuations in HCT116 cells varied depending on the UVA dose and were inversely correlated with those in control cells after proliferation-inhibiting doses, but were positively correlated after proliferation-stimulating doses. In HCT116 cells the DCFH-DA-detected ROS level changed more regularly than that in Me45 cells, while in Me45 cells irradiated with proliferation-inhibiting UVA doses it became inversely correlated compared to the dynamics in control cells. An increase of proliferation rate after irradiation was observed only if the fluctuations of ROS level retained their pattern in control cells, although conservation of the pattern of fluctuations of different radicals in both cell lines were important (Table 1). Overall, these results suggest that it is the pattern of fluctuations of radical levels, rather than the levels themselves, which

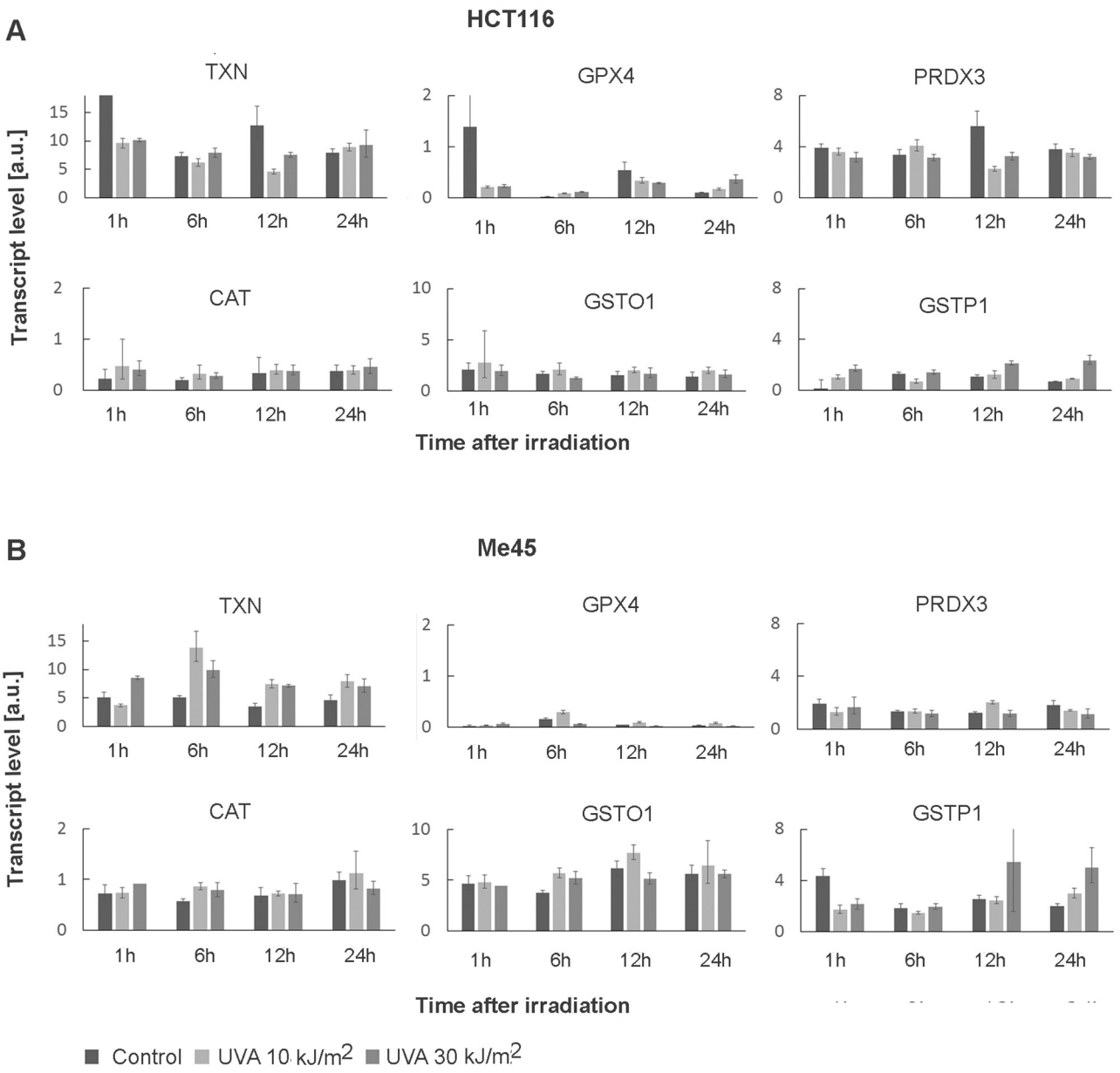

Fig 5. Changes of expression after UVA radiation (10kJ/m^2, 30kJ/m^2) and control cells. Results are presented as relative level to RPL41 transcript expression with standard deviation.

https://doi.org/10.1371/journal.pone.0205215.g005

influences proliferation rate after UVA irradiation and that each cell type may use different pathways to regulate cellular redox status.

ROS-regulating pathways and their choice in HCT116 and Me45 cells

ROS participate in many signaling pathways, including those regulating the cell cycle and proliferation [9, 20, 22, 24], and their intracellular levels must be precisely controlled. The main players in regulation of cellular redox status are superoxide and NO which are produced by cells and interact with each other and with many other cellular molecules. Their levels are regulated by a series of feedback circuits, mainly based on peroxiredoxins, thioredoxins,

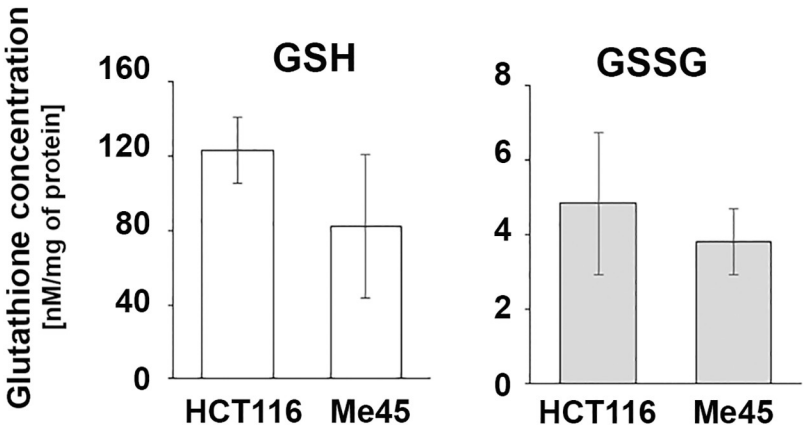

Fig 6. Levels of reduced (GSH) and oxidized (GSSG) glutathione in HCT116 and Me45 cells. Data show the mean and SD of 3 independent experiments.

https://doi.org/10.1371/journal.pone.0205215.g006

glutathione, thioredoxin and glutathione reductases, NADPH, and enzymes engaged in production of superoxide or NO [53, 54, 55] (Fig 7). Fig 7 shows some proteins whose differential expression in Me45 and HCT116 cells may influence these pathways. Many other possible interactions of superoxide and $ONOO^-$ occur, with themselves, with other proteins, CO_2, antioxidants, and other compounds which result in creation of new radicals and interaction circuits which further influence the redox state of the cell and create additional regulatory subcircuits, described in detail in many recent and older reviews [53, 55, 56, 57]. Nevertheless, the ROS regulatory circuits in Fig 7 seem to create the basic pathways for redox regulation in cells which may determine the character of radical level fluctuations.

The two main pathways leading to regulation of superoxide levels start by its conversion to H_2O_2 or to peroxynitrite in reactions with NO [55, 58]. H_2O_2 may be created by interaction of two superoxide molecules, either spontaneously or more efficiently by superoxide dismutase (SOD) [22, 24, 58]. Interaction of superoxide with NO starts another pathway by creation of the very reactive peroxynitrite radical ($ONOO^-$); the sources of superoxide and NO and their spatial separation may determine further regulatory pathways through H_2O_2 or $ONOO^-$ in cells.

NOS produces either NO or superoxide in appropriate conditions [59], and we speculate that this could explain the more frequent colocalization of these two types of radical in Me45 than in HCT116 cells (Fig 4). This hypothesis is supported by data confirming presence of NOS in mitochondria. The NOS3 (eNOS) protein has been identified in the membrane of mitochondria from skeletal muscle, brain, heart and kidney [60, 61, 62, 63]. Also presence of iNOS (NOS2) has been showed in mitochondrial fraction [64]. Several groups claimed that mitochondria contain specific NOS form (mtNOS) similar to nNOS (NOS1) and/or eNOS. It is controversial as some results suggest that mtNOS is in fact nNOS or eNOS, however there are strong evidence of NOS presence in mitochondria [63, 65, 66].

All isoforms of NOS contain the N-terminal oxygenase and C-terminal reductase domains separated by a linker, and function as homodimers which produce NO by oxidation of L-arginine to L-citrulline [67, 68, 69]. In the absence of the cofactor, tetrahydrobiopterin (BH4), the domains become uncoupled and NOS produces superoxide instead of NO [47, 48, 68, 69]. The levels of transcripts for the NOS isoforms are rather low and are similar in HCT116 and Me45 cells, except that for NOS2 which is slightly higher in HCT116 cells (Table 3 and S2 Table). However, the gene *GCH1* which encodes the rate-limiting enzyme in synthesis of BH4 [70] is

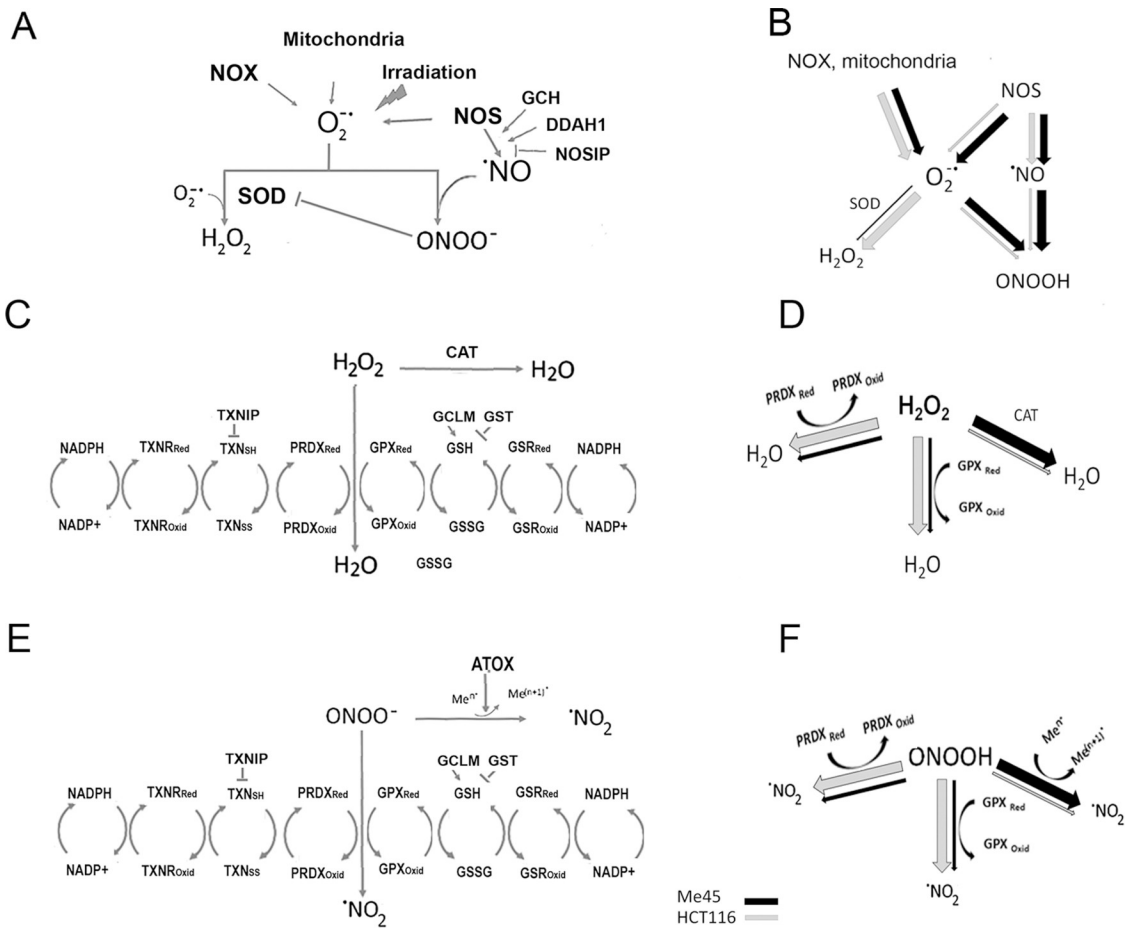

Fig 7. The main pathways for regulation of superoxide and NO levels in Me45 and HCT116 cells. A,C and E show production and further interactions of superoxide (A), hydrogen peroxide (C) and peroxynitrite (E) and regulatory pathways engaged. B,D and F compare use of presented regulatory pathways in HCT116 and Me45 cells by the size of black (Me45) and white (HCT116) arrows.

https://doi.org/10.1371/journal.pone.0205215.g007

expressed at a significantly lower level in Me45 cells (Table 3) which could result in insufficient availability of BH4 and consequently an increased production of superoxide by NOS. Further, in Me45 cells the level of transcripts for glutathione transferases is significantly higher (Table 2) and glutathionylation of NOS results in increased production of superoxide [48, 71]. Either or both of these scenarios would result in superoxide forming a larger fraction of the products of NOS in Me45 cells and to the observed more frequent apparent colocalization with NO. This would lead to higher production of peroxynitrite which may be further converted to NO_2 by peroxiredoxins and glutathione peroxidases which also participate in reduction of H_2O_2 [72, 73] and these pathways are probably used preferentially by HCT116 cells which show higher expression of PRDX, TXN, GPX than Me45 cells. The other pathway for ONOO- reduction is interaction with transition metal centers (reviewed in [53]) and Me45 cells show significantly higher levels than HCT116 cells of *ATOX* gene transcripts coding for copper chaperone [22, 74] and of transcripts of thioredoxin-inhibiting protein TXNIP, suggesting that in Me45 cells interaction of $ONOO^-$ with transition metals may be dominating.

Glutathione is a further important player in redox regulation, and its level is lower in Me45 cells than in HCT116 cells (Fig 6). This could plausibly be due to the lower expression of the *GCLM* gene (Table 3), or to greater use of glutathione for glutathionylation of proteins since

genes coding for GSTs are more highly expressed in Me45 cells. As glutathione is necessary for reactivation of GPX, one could again expect that the pathway engaging GPX will be also less efficient in Me45 cells.

Redox balance plays a critical role in regulating biological processes and many cellular pathways, including stimulation and inhibition of proliferation, are influenced by ROS levels. Our results suggest that cells may concentrate on strict regulation of superoxide or hydrogen peroxide levels when changed by stress, and that stimulation or inhibition of cell proliferation depend on the dynamics of level fluctuations and less on the ROS levels themselves. We show for the first time that varying responses of different cell types to the same stimulus such as a specific dose of UVA may result from their use of different redox control pathways. Existence of such alternative pathways of redox environment control in different cell lines may have implication for therapies using UV as well as further studies of cellular response to stress factors.

Supporting information

S1 Table.
(DOCX)

S2 Table. Expression of genes engaged in redox processes in Me45 and HCT116 cells.
(DOCX)

Acknowledgments

This work was supported by the Polish National Science Center Grant 2015/19/B/ST7/02984.

Ronald Hancock (Laval University, Québec, Canada) is acknowledged for critically reading and editing the manuscript.

Author Contributions

Conceptualization: Sylwia Ciesielska, Joanna Rzeszowska-Wolny.

Formal analysis: Sylwia Ciesielska, Dorota Hudy.

Funding acquisition: Joanna Rzeszowska-Wolny.

Investigation: Sylwia Ciesielska, Patryk Bil, Karolina Gajda, Aleksandra Poterala-Hejmo, Dorota Hudy.

Methodology: Patryk Bil, Aleksandra Poterala-Hejmo.

Project administration: Joanna Rzeszowska-Wolny.

Software: Patryk Bil.

Writing – original draft: Sylwia Ciesielska, Joanna Rzeszowska-Wolny.

Writing – review & editing: Joanna Rzeszowska-Wolny.

References

1. IARC Working Group Reports. Vol 1. Exposure to artificial UV radiation and skin cancer. ISBN 92 832 2441 8, 2005
2. Sluyter R, Halliday GM. Enhanced tumor growth in UV-irradiated skin is associated with an influx of inflammatory cells into the epidermis. Carcinogenesis. 2000; 21: 1801–1807 PMID: 11023536

3. Han CY, Hien TT, Lim SC, Kang KW. Role of Pin1 in UVA-induced cell proliferation and malignant transformation in epidermal cells. Biochem Biophys Res Commun. 2011; 410: 68–74 https://doi.org/10.1016/j.bbrc.2011.05.106 PMID: 21640077
4. Bachelor MA, Bowden GT. UVA-mediated activation of signaling pathways involved in skin tumor promotion and progression. Semin Cancer Biol. 2004; 14:131–8 https://doi.org/10.1016/j.semcancer.2003.09.017 PMID: 15018897
5. Berton TR, Mitchell DL, Fischer SM, Locniskar MF. Epidermal proliferation but not quantity of DNA photodamage is correlated with UV-induced mouse skin carcinogenesis. J Invest Dermatol. 1997; 109:3407
6. Liu Z, Chen H, Yang H, Liang J, Li X. Low-Dose UVA Radiation-Induced Adaptive Response in Cultured Human Dermal Fibroblasts. International Journal of Photoenergy. 2012; ID 167425.
7. WHO. Global Solar UV index. ISBN 92 4 159007 6, 2002
8. El-Abaseri TB, Putta S, Hansen LA. Ultraviolet irradiation induces keratinocyte proliferation and epidermal hyperplasia through the activation of the epidermal growth factor receptor. Carcinogenesis. 2006; 27:225–31 https://doi.org/10.1093/carcin/bgi220 PMID: 16123117
9. Grossman N, Schneid N, Reuveni H, Halevy S, Lubart R. 780 nm low power diode laser irradiation stimulates proliferation of keratinocyte cultures: involvement of reactive oxygen species. Lasers Surg Med. 1998; 22: 212–8 PMID: 9603282
10. Kannouche P, Pinon-Lataillade G, Tissier A, Chevalier-Lagente O, Sarasin A,Mezzina M, et al. The nuclear concentration of kin17, a mouse protein that binds to curved DNA, increases during cell proliferation and after UV irradiation. Carcinogenesis. 1998; 19: 781–9 PMID: 9635863
11. Staberg B, Wulf HC, Klemp P, Poulsen T, Brodthagen H. The carcinogenic effect of UVA irradiation. Journal of Investigative Dermatology. 1983; 81: 517–519 PMID: 6644093
12. Bossi O, Gartsbein M, Leitges M, Kuroki T, Grossman S, Tennenbaum T. UV irradiation increases ROS production via PKCdelta signaling in primary murine fibroblasts. J Cell Biochem. 2008; 105: 194–207 https://doi.org/10.1002/jcb.21817 PMID: 18523985
13. Aguirre J, Lambeth JD. Nox enzymes from fungus to fly to fish and what they tell us about Nox function in mammals. Free Radic Biol Med. 2010; 49:1342–53 https://doi.org/10.1016/j.freeradbiomed.2010.07.027 PMID: 20696238
14. Burdon RH. Superoxide and hydrogen peroxide in relation to mammalian cell proliferation. Free Radic Biol Med. 1995; 18:775–94 PMID: 7750801
15. Foksinski M, Zarakowska E, Gackowski D, Skonieczna M, Gajda K, Hudy D, et al. Profiles of a broad spectrum of epigenetic DNA modifications in normal and malignant human cell lines: Proliferation rate is not the major factor responsible for the 5-hydroxymethyl-2'-deoxycytidine level in cultured cancerous cell lines. PLoS One. 2017; 12: e0188856 https://doi.org/10.1371/journal.pone.0188856 PMID: 29190698
16. Irani K. Oxidant signaling in vascular cell growth, death, and survival: a review of the roles of reactive oxygen species in smooth muscle and endothelial cell mitogenic and apoptotic signaling. Circ Res. 2000; 87: 179–83 PMID: 10926866
17. Jaksik R, Lalik A, Skonieczna M, Cieslar-Pobuda A, Student S, Rzeszowska-Wolny J. MicroRNAs and reactive oxygen species: are they in the same regulatory circuit? Mutat Res Genet Toxicol Environ Mutagen. 2014; 764–765: 64–71 https://doi.org/10.1016/j.mrgentox.2013.09.003 PMID: 24051449
18. Janssen Y, Van Houten B, Borm P, Mossman B. Cell and tissue responses to oxidative damage. Lab Investig. 1993; 69: 261–274 PMID: 8377469
19. Klotz LO, Pellieux C, Briviba K, Pierlot C, Aubry JM, Sies H. Mitogen activated protein kinase (p38-, JNK-, ERK-) activation pattern induced by extracellular and intracellular singlet oxygen and UVA. Eur J Biochem. 1999; 260: 917–22 PMID: 10103024
20. Menon SG, Goswami PC. A redox cycle within the cell cycle: ring in the old with the new. Oncogene. 2007; 26: 1101–9 https://doi.org/10.1038/sj.onc.1209895 PMID: 16924237
21. Murrell GA, Francis MJ, Bromley L. Modulation of fibroblast proliferation by oxygen free radicals. Biochem J. 1990; 265: 659–65 PMID: 2154966
22. Sarsour EH, Kumar MG, Chaudhuri L, Kalen AL, Goswami PC. Redox control of the cell cycle in health and disease. Antioxid Redox Signal. 2009; 11: 2985–3011 https://doi.org/10.1089/ARS.2009.2513 PMID: 19505186
23. Skonieczna M, Hejmo T, Poterala-Hejmo A, Cieslar-Pobuda A, and Buldak RJ. NADPH oxidases: Insights into selected functions and mechanisms of action in cancer and stem cells. Oxidative Medicine and Cellular Longevity. 2017; vol. 2017

24. Boonstra J, Post JA. Molecular events associated with reactive oxygen species and cell cycle progression in mammalian cells. Gene. 2004; 337:1–13 https://doi.org/10.1016/j.gene.2004.04.032 PMID: 15276197

25. Hatanaka E, Dermargos A, Armelin HA, Curi R, Campa A. Serum amyloid A induces reactive oxygen species (ROS) production and proliferation of fibroblast. Clin Exp Immunol. 2011; 163: 362–7 https://doi.org/10.1111/j.1365-2249.2010.04300.x PMID: 21175596

26. Villalobo A. Nitric oxide and cell proliferation. FEBS J. 2006; 273: 2329–44 https://doi.org/10.1111/j.1742-4658.2006.05250.x PMID: 16704409

27. Ignarro LJ, Buga GM, Wei LH, Bauer PM, Wu G, del Soldato P. Role of the arginine-nitric oxide pathway in the regulation of vascular smooth muscle cell proliferation. Proc Natl Acad Sci USA. 2001; 8: 4202–8

28. Napoli C, Paolisso G, Casamassimi A, Al-Omran M, Barbieri M, Sommese L, et al. Effects of nitric oxide on cell proliferation: novel insights. J Am Coll Cardiol. 2013; 62: 89–95 https://doi.org/10.1016/j.jacc.2013.03.070 PMID: 23665095

29. Finkel T. Signal transduction by mitochondrial oxidants. J Biol Chem. 2012; 287: 4434–40 https://doi.org/10.1074/jbc.R111.271999 PMID: 21832045

30. Trachootham D, Lu W, Ogasawara MA, Nilsa RD, Huang P. Redox regulation of cell survival. Antioxid Redox Signal. 2008; 10: 1343–74 https://doi.org/10.1089/ars.2007.1957 PMID: 18522489

31. da Veiga Moreira J, Peres S, Steyaert JM, Bigan E, Paulevé L, Nogueira ML, et al. Cell cycle progression is regulated by intertwined redox oscillators. Theor Biol Med Model. 2015; 12:10 https://doi.org/10.1186/s12976-015-0005-2 PMID: 26022743

32. Thomas DD, Ridnour LA, Isenberg JS, Flores-Santana W, Switzer CH, Donzelli S, et al. The chemical biology of nitric oxide: implications in cellular signaling. Free Radic Biol Med. 2008; 45:18–31 https://doi.org/10.1016/j.freeradbiomed.2008.03.020 PMID: 18439435

33. Krzywon A, Widel M, Fujarewicz K, Skonieczna M, Rzeszowska-Wolny J. Modulation by neighboring cells of the responses and fate of melanoma cells irradiated with UVA. J Photochem Photobiol B. 2018; 178: 505–511 https://doi.org/10.1016/j.jphotobiol.2017.12.012 PMID: 29241122

34. Robinson KM, Janes MS, Beckman JS. The selective detection of mitochondrial superoxide by live cell imaging Nat Protoc. 2008; 3: 941–47 https://doi.org/10.1038/nprot.2008.56

35. Robinson KM, Janes MS, Pehar M, Monette JS, Ross MF, Hagen TM, et al. Selective fluorescent imaging of superoxide in vivo using ethidium-based probes. Proc Natl Acad Sci USA. 2006; 103: 15038–43 https://doi.org/10.1073/pnas.0601945103 PMID: 17015830

36. Wilson CL, Miller CJ. Simpleaffy: a BioConductor package for Affymetrix Quality Control and data analysis. Bioinformatics. 2005; 21: 3683–3685 https://doi.org/10.1093/bioinformatics/bti605 PMID: 16076888

37. Dai M, Wang P, Boyd AD, Kostov G, Athey B, Jones EG, et al. Evolving gene/transcript definitions significantly alter the interpretation of GeneChip data. Nucleic Acids Research. 2005; 33: e175 https://doi.org/10.1093/nar/gni179 PMID: 16284200

38. Irizarry RA, Bolstad BM, Collin F, Cope LM, Hobbs B, Speed TP. Summaries of Affymetrix GeneChip probe level data. Nucleic Acids Research. 2003; 31:e15 PMID: 12582260

39. Rahman I, Kode A, Biswas SK. Assay for quantitative determination of glutathione and glutathione disulfide levels using enzymatic recycling method. Nat Protoc 1: 3159–31645, https://doi.org/10.1038/nprot.2006.378 PMID: 17406579

40. Vandeputte C, Guizon I, Genestie-Denis I, Vannier B, Lorenzon G. A microtiter plate assay for total glutathione and glutathione disulfide contents in cultured/isolated cells: performance study of a new miniaturized protocol. Cell Biology and Toxicology. 1994; 10: 415–421 PMID: 7697505

41. Ye J, Coulouris G, Zaretskaya I, Cutcutache I, Rozen S, Madden T. Primer-BLAST: A tool to design target-specific primers for polymerase chain reaction. BMC Bioinformatics. 2012; 13:134 https://doi.org/10.1186/1471-2105-13-134 PMID: 22708584

42. Owczarzy R, Tataurov AV, Wu Y, Manthey JA, McQuisten KA, Almabrazi HG, et al. IDT SciTools: a suite for analysis and design of nucleic acid oligomers. Nucleic Acids Res. 2008; 36:W163–9 https://doi.org/10.1093/nar/gkn198 PMID: 18440976

43. Ubezio P, Civoli F. Flow cytometric detection of hydrogen peroxide production induced by doxorubicin in cancer cells. Free Radic Biol Med. 1994; 16: 509–16 PMID: 8005536

44. Arnold RS, Shi J, Murad E, Whalen AM, Sun CQ, Polavarapu R, et al. Hydrogen peroxide mediates the cell growth and transformation caused by the mitogenic oxidase Nox1. Proc Natl Acad Sci U S A. 2001; 98:5550–5 https://doi.org/10.1073/pnas.101505898 PMID: 11331784

45. Culotta VC, Yang M, O'Halloran TV. Activation of superoxide dismutases: putting the metal to the pedal. Biochim Biophys Acta. 2006; 1763: 747–758 https://doi.org/10.1016/j.bbamcr.2006.05.003 PMID: 16828895

46. Ozumi K, Sudhahar V, Kim H-W, Chen G-F, Kohno T, Finney L, et al. Role of copper transport protein antioxidant 1 in angiotensin II–induced hypertension a key regulator of extracellular superoxide dismutase. Hypertension. 2012; 60: 476–486 https://doi.org/10.1161/HYPERTENSIONAHA.111.189571

47. Benson MA, Batchelor H, Chuaiphichai S, Bailey J, Zhu H, Stuehr DJ, et al. A pivotal role for tryptophan 447 in enzymatic coupling of human endothelial nitric oxide synthase (eNOS): effects on tetrahydrobiopterin-dependent catalysis and eNOS dimerization. J Biol Chem. 2013; 288: 29836–45 https://doi.org/10.1074/jbc.M113.493023 PMID: 23965989

48. Crabtree MJ, Brixey R, Batchelor H, Hale AB, Channon KM. Integrated redox sensor and effector functions for tetrahydrobiopterin- and glutathionylation-dependent endothelial nitric-oxide synthase uncoupling. J Biol Chem. 2013; 288:561–9 https://doi.org/10.1074/jbc.M112.415992 PMID: 23139420

49. Burdon RH, Gill V, Rice-Evans C. Cell proliferation and oxidative stress. Free Radic Res Commun. 1989; 7:149–59 PMID: 2511085

50. Ikebuchi Y, Masumoto N, Tasaka K, Koike K, Kasahara K, Miyake A, et al. Superoxide anion increases intracellular pH, intracellular free calcium, and arachidonate release in human amnion cells. J Biol Chem. 1991; 266: 13233–7 PMID: 1649184

51. Burdon RH. Control of cell proliferation by reactive oxygen species. Biochem Soc Trans. 1996; 24:1028–32 PMID: 8968506

52. Forman HJ. Redox signaling: An evolution from free radicals to aging. Free Radic Biol Med. 2016; 97:398–407 https://doi.org/10.1016/j.freeradbiomed.2016.07.003 PMID: 27393004

53. Bartesaghi S, Radi R. Fundamentals on the biochemistry of peroxynitrite and protein tyrosine nitration. Redox Biol. 2018; 14:618–625 https://doi.org/10.1016/j.redox.2017.09.009 PMID: 29154193

54. Hanschmann EM, Godoy JR, Berndt C, Hudemann C, Lillig CH. Thioredoxins, glutaredoxins, and peroxiredoxins—molecular mechanisms and health significance: from cofactors to antioxidants to redox signaling. Antioxid Redox Signal. 2013; 19: 1539–605 https://doi.org/10.1089/ars.2012.4599

55. Radi R. Peroxynitrite, a stealthy biological oxidant. J Biol Chem. 2013; 288: 26464–72 https://doi.org/10.1074/jbc.R113.472936 PMID: 23861390

56. Radi R. Nitric oxide, oxidants, and protein tyrosine nitration. Proc Natl Acad Sci U S A. 2004; 101: 4003–8 https://doi.org/10.1073/pnas.0307446101 PMID: 15020765

57. Szabo C, Ischiropoulos H, Radi R. Peroxynitrite: biochemistry, pathophysiology and development of therapeutics. Nature Rev. Drug Discovery. 2007; 6: 662–680

58. Beckman JS, Koppenol WH. Nitric oxide, superoxide, and peroxynitrite: the good, the bad, and ugly. Am J Physiol. 1996; 271: C1424–37 https://doi.org/10.1152/ajpcell.1996.271.5.C1424 PMID: 8944624

59. Radi R, Cassina A, Hodara R. Nitric oxide and peroxynitrite interactions with mitochondria, Biol Chem. 2001; 383:401–409

60. Bates TE, Loesch A, Burnstock G, Clark JB. Mitochondrial Nitric Oxide Synthase: A Ubiquitous Regulator of Oxidative Phosphorylation? Biochem. Biophys. Res. Commun., 1996; 218: 40–44 https://doi.org/10.1006/bbrc.1996.0008 PMID: 8573169

61. Bates TE, Loesch A, Burnstock G, Clark JB. Immunocytochemical Evidence for a Mitochondrially Located Nitric Oxide Synthase in Brain and Liver. Biochem. Biophys. Res. Commun., 1995; 213: 896–900 https://doi.org/10.1006/bbrc.1995.2213 PMID: 7544582

62. Reiner M, Bloch W, Addicks K. Functional Interaction of Caveolin-1 and eNOS in Myocardial Capillary Endothelium Revealed by Immunoelectron Microscopy. J. Histochem. Cytochem., 2001; 49: 1605–1609 https://doi.org/10.1177/002215540104901214 PMID: 11724908

63. Lacza Z, Puskar M, Figueroa JP, Zhang J, Rajapakse N, Busija DW. Mitochondrial nitric oxide synthase is constitutively active and is functionally upregulated in hypoxia. Free Radic. Biol. Med., 2001; 31: 1609–1615 PMID: 11744335

64. Chen K, Northington FJ, Martin LJ. Inducible nitric oxide synthase is present in motor neuron mitochondria and Schwann cells and contributes to disease mechanisms in ALS mice. Brain Struct. Funct., 2010; 214: 219–234 https://doi.org/10.1007/s00429-009-0226-4 PMID: 19888600

65. Kanai AJ, Pearce LL, Clemens PR, Birder LA, VanBibber MM, Choi S-Y, et al. Identification of a neuronal nitric oxide synthase in isolated cardiac mitochondria using electrochemical detection. Proc. Natl. Acad. Sci., 2001; 98: 14126 LP–14131

66. Ghafourifar P, Cadenas E. Mitochondrial nitric oxide synthase., Trends Pharmacol. Sci., 2005; 26: 190–195 https://doi.org/10.1016/j.tips.2005.02.005 PMID: 15808343

67. Pou S, Pou WS, Bredt DS, Snyder SH, Rosen GM. Generation of superoxide by purified brain nitric oxide synthase. J Biol Chem. 1992; 267: 24173–6 PMID: 1280257

68. Forstermann U, Sessa WC. Nitric oxide synthases. Regulation and function. Eur. Heart J. 2012; 33: 829–837 https://doi.org/10.1093/eurheartj/ehr304 PMID: 21890489

69. Vásquez-Vivar J, and Kalyanaraman B. Generation of superoxide from nitric oxide synthase. FEBS Lett. 2000; 481: 305–306 PMID: 11041680

70. Cai S, Alp NJ, McDonald D, Smith I, Kay J, Canevari L, et al. GTP cyclohydrolase I gene transfer augments intracellular tetrahydrobiopterin in human endothelial cells: effects on nitric oxide synthase activity, protein levels and dimerisation. Cardiovasc Res. 2002; 55: 838–49 PMID: 12176133

71. Chen CA, Wang TY, Varadharaj S, Reyes LA, Hemann C, Talukder MA, et al. S-glutathionylation uncouples eNOS and regulates its cellular and vascular function. Nature. 2010; 468:1115–1118 https://doi.org/10.1038/nature09599 PMID: 21179168

72. Knoops B, Goemaere J, Van der Eecken V, Declercq JP. Peroxiredoxin 5: structure, mechanism, and function of the mammalian atypical 2-Cys peroxiredoxin. Antioxid Redox Signal. 2011; 15: 817–29 https://doi.org/10.1089/ars.2010.3584 PMID: 20977338

73. Walbrecq G, Wang B, Becker S, Hannotiau A, Fransen M, Knoops B. Antioxidant cytoprotection by peroxisomal peroxiredoxin-5. Free Radic Biol Med. 2015; 84: 215–226 https://doi.org/10.1016/j.freeradbiomed.2015.02.032 PMID: 25772011

74. Hatori Y, Inouye S, Akagi R. Thiol-based copper handling by the copper chaperone Atox1. IUBMB Life. 2017; 69: 246–254 https://doi.org/10.1002/iub.1620 PMID: 28294521